Received: 5 November 2024 | Revised: 5 February 2025 | Accepted: 22 May 2025

DOI: 10.1111/php.70000

RESEARCH ARTICLE

Developing giant plasma membrane vesicles from *Leishmania* cells to investigate the role of membrane proteins in photodynamic inactivation

Maressa D. F. de Souza[1] | **Pietro Ciancaglini**[2] | **Rosangela Itri**[3] | **Martha S. Ribeiro**[1]

[1]Centro de Lasers e Aplicações, Instituto de Pesquisas Energéticas e Nucleares (IPEN-CNEN), São Paulo, Brazil

[2]Departamento de Química, Faculdade de Filosofia, Ciências e Letras de Ribeirão Preto, Universidade de São Paulo, Ribeirão Preto, Brazil

[3]Departmento de Física Aplicada, Instituto de Física, Universidade de São Paulo, São Paulo, Brazil

Correspondence
Rosangela Itri, Instituto de Física, Universidade de São Paulo, Rua do Matão, 1371, 05508-090, São Paulo, SP, Brazil.
Email: itri@if.usp.br

Martha S. Ribeiro, Center for Lasers and Applications, IPEN-CNEN, Av. Lineu Prestes, 2242, 05508-000, São Paulo, SP, Brazil.
Email: marthasr@usp.br

Funding information
Conselho Nacional de Desenvolvimento Científico e Tecnológico, Grant/Award Number: 465763/2014-6; Comissão Nacional de Energia Nuclear; Coordenação de Aperfeiçoamento de Pessoal de Nível Superior, Grant/Award Number: 001

Abstract

Interest in antimicrobial photodynamic therapy for treating cutaneous leishmaniasis has been rising, showing promising outcomes and good patient tolerance. In this study, we aimed to develop a protocol for producing giant plasma membrane vesicles (GPMVs) from *Leishmania amazonensis* promastigote cell membranes, focusing on the role of membrane-embedded proteins during methylene blue (MB) photooxidation with red light. Membrane extraction was achieved via centrifugation with various sucrose gradients. We then generated GPMVs by electroformation, applying different frequencies and voltages over four cycles, and examined them using phase contrast optical microscopy. For MB photooxidation, GPMVs were dispersed in an aqueous solution with 50 μM MB and exposed to 665 nm light at 830 μW. A comparable approach was used for mimetic membranes (giant unilamellar vesicles, GUVs) made of *Leishmania* membrane lipids. MB photoactivation in GUVs caused a transient increase in membrane area and full permeability. Conversely, GPMVs showed an earlier onset of contrast loss but exhibited less overall contrast reduction and no expansion, indicating that membrane proteins in GPMVs modulate the response to oxidative stress. Real-time monitoring revealed morphological changes in *L. amazonensis* promastigote cells consistent with apoptosis following photodynamic inactivation.

KEYWORDS

Leishmania amazonensis, membrane biophysics, methylene blue, optical contrast, photooxidation, red light

Abbreviations: aPDT, antimicrobial photodynamic therapy; DOPC, 1,2-dioleoyl-sn-glycero-3-phosphocholine; ERG, ergosterol; GPMVs, giant plasm membrane vesicles; GUVs, giant unilamellar vesicles; ICP, inositol phosphorylceramide; ITO, indium titanium oxide; MB, methylene blue; PBS, phosphate-buffered saline; PC, phosphatidylcholine; PDI, photodynamic inactivation; PE, phosphatidylethanolamine; PI, phosphatidylinositol; PLs, phospholipids; POPC, 1-palmitoyl-2-oleoyl-sn-glycerol-3-phosphocholine; POPE, 1-palmitoyl-2-oleoyl-sn-glycerol-phosphoethanolamine; PS, photosensitizer; ROS, reactive oxygen species; SDS-PAGE, sodium dodecyl-sulfate polyacrylamide gel electrophoresis; SL, sphingolipids; SM, sphingomyelin.

INTRODUCTION

Antimicrobial photodynamic therapy (aPDT) or photodynamic inactivation (PDI, for in vitro studies) is an innovative technique that utilizes light-sensitive compounds known as photosensitizers (PSs), which, when activated by specific wavelengths of light, generate reactive oxygen species (ROS) capable of killing viruses, bacteria, fungi, and parasites. This non-invasive approach offers a promising alternative to traditional antimicrobials, particularly in addressing multidrug-resistant pathogens. The key mechanisms of aPDT involve the application of a PS to the target area, which, when exposed to light, typically in the visible range, becomes activated from its ground state to an excited singlet state. The excited PS then transfers energy to molecular oxygen (Type II reaction) or transfers charge directly to cellular components (Type I reaction). Both processes result in the production of ROS, which attack key microbial structures, including the cell wall, membrane, and internal components such as DNA and proteins, leading to cell death.[1]

It is well known that the cell membrane is the first target of PDI. Previous works based on lipid oxidation promoted by photoactivation of PSs in model lipid membranes revealed that lipid oxidation may cause changes in membrane surface area, permeability increase, membrane disruption, and changes in membrane lipid domains.[2–4] All these effects depend on the membrane lipid composition and type of produced photooxidized lipids, which are related to PS features, such as the generation of singlet oxygen ($^1O_2$) and other ROS, as well as their location in the membrane.[5] For instance, it has been previously shown that membrane permeabilization is faster for 1,2-dioleoy l-*sn*-glycero-3-phosphocholine (DOPC) lipid membrane (that contains one unsaturation in each alkyl chain) following methylene blue (MB) photoactivation than for 1-palmitol-2-oleoyl-sn-glycerol-3-phosphocholine (POPC) lipid membrane (just one unsaturation in one of the alkyl chains).[3] However, the role of photooxidation in more complex in giant unilamellar vesicles (GUVs) and giant plasm membrane vesicles (GPMVs) remains unexplored.

Here, we focus our attention on investigating how photooxidation may impact reconstituted parasite membranes, as leishmaniasis (a parasitic neglected disease transmitted by the bite of an insect vector) shows good results following aPDT.[6,7] This disease primarily affects people in low-income countries, where poor housing, inadequate hygiene, and limited access to healthcare are common. However, due to high population mobility and climate change, it is estimated that more than 1 million new cases occur globally each year.[8]

The membrane content of *Leishmania* spp. is rich in phospholipids (PLs) and sphingolipids (SLs).[9] The most abundant PL is phosphatidylcholine (PC) followed by phosphatidylethanolamine (PE) and phosphatidylinositol (PI). On the other hand, the main SL is inositol phosphorylceramide (ICP) instead of sphingomyelin (SM) like in mammals.[10] Additionally, *Leishmania* spp. present ergosterol (ERG) in their membrane rather than cholesterol.[10]

In the current work, we prepared GUVs that mimic the lipid bilayer model for *Leishmania* spp. Further, we developed a protocol to produce GPMVs from *Leishmania amazonensis* cells. The latter is characterized by the presence of membrane-embedded proteins. Both GUVs and GPMVs dispersed in MB solutions upon irradiation were observed by phase contrast optical microscopy. We evaluated the dynamics of the photodamage on the vesicles through changes in the membrane surface area and permeability. At last, we monitored the real-time killing of *L. amazonensis* promastigote cells by PDI.

MATERIALS AND METHODS

Preparation of GUVs

For model lipid membranes, POPC, 1-palmitoyl-2-oleoyl -sn-glycerol-phosphoethanolamine (POPE), SM (porcine brain, Avanti Polar Lipids, Inc., USA), and ERG (Sigma-Aldrich, USA) were used. Model lipid membranes represented by GUVs were prepared with POPC:POPE:SM:ERG in the molar ratio 45:10:15:30. Here, SM replaced ICP since ICP is not commercially available. GUVs formed by POPC:POPE:SM:ERG mimic the lipid bilayer of the plasma membrane of parasites of the genus *Leishmania*.[10]

The preparation of the GUVs was carried out using the traditional method of electroformation.[11] Briefly, 10-μL of a 2 mM total lipid solution in chloroform was spread on the surfaces of two conductive glasses coated with indium titanium oxide (ITO, Sigma-Aldrich, USA), which were then placed with their conductive sides facing each other, separated by a 2 mm thick Teflon frame. This electro swelling chamber was filled with 0.2 M sucrose solution previously measured in an osmometer (Osmoma Gonotec 030, Germany), and connected to an alternating power generator (Minipa MFG-4201A, Korea) at 1.5 V and 10 Hz frequency during 1.5 h at a temperature of 50°C (in an oven), above the SM gel-phase transition. Afterward, the vesicle solution was carefully transferred to an Eppendorf vial and held at rest at 4°C before use.

L. amazonensis membrane isolation

To isolate the membrane of *L. amazonensis*, we employed the membrane separation protocol developed

by Mukherjee et al.[12] This protocol utilizes a hypotonic buffer, followed by vortexing and the separation of various cellular components through sucrose gradient centrifugation. However, we made several adjustments to enhance the separation process, particularly modifying the washing steps, as detailed below.

L. amazonensis promastigote cells (MHOM/BR/73/M2269) were cultured in 80% M199 medium (Sigma-Aldrich, USA) and 20% fetal bovine serum (Gibco TM Invitrogen Corporation, USA) at a temperature of 25°C. After 7 days, parasites were centrifuged at 3000 *g* for 10 min; the supernatant was removed and discarded. The pellet was then transferred to another tube, which was centrifuged for 10 min at 3000 *g*. Thereafter, the supernatant was discarded, and the pellet was solubilized in 1 mL of 5 mM Tris–HCl buffer solution together with 0.5 mM of protease inhibitor cocktail. The solution was put in the refrigerator at a temperature of 4°C for 90 min, stirring every 10 min on a vortex. In the last agitation process, 2 mM of calcium chloride was added to the solution, followed by 20 min centrifugation at 3300 *g*. Then, the pellet was dissolved in a 5% (w/v) sucrose solution, previously prepared in 50 mM Tris–HCl buffer. In a tube, 10 mL of 20% sucrose diluted in Tris–HCl buffer was added, followed by the sample solution in 5% sucrose, forming two distinct phases. The tube was centrifuged at 1500 *g* for 30 min at 4°C. The process was repeated 4 times to separate the plasma membrane from the parasite cell (Figure 1A).

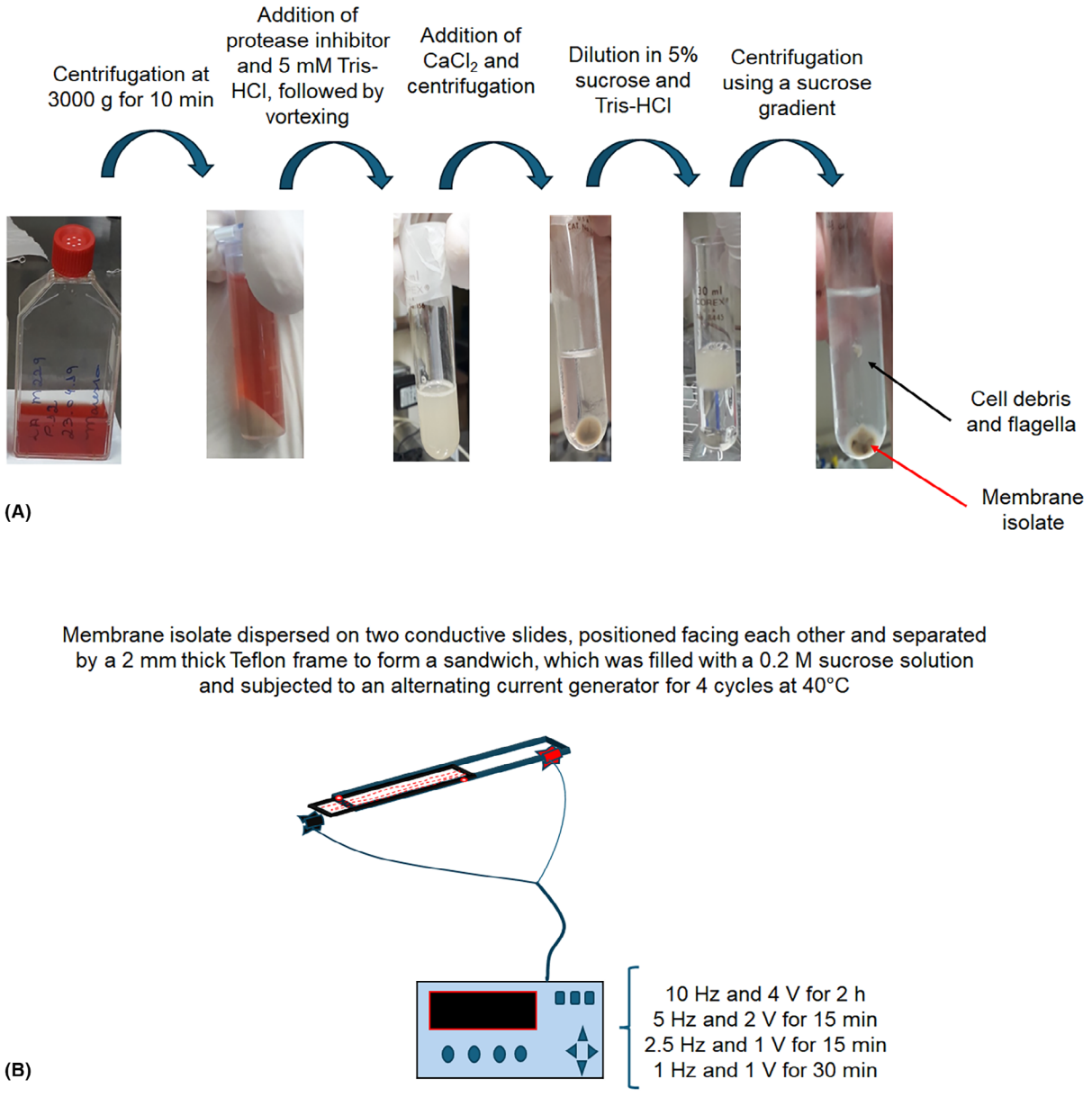

FIGURE 1 Schematic illustration of the protocol for isolating the plasma membrane from *L. amazonensis* promastigote cells (A) and GPMV reconstitution (B).

L. amazonensis membrane reconstitution in GPMVs

GPMVs were grown by the electroformation method under heating with voltage and frequency variation. On the top of two conductive slides, which were coated with ITO, 20 μL of the membrane isolate was added. The slides were then taken to a desiccator connected to a vacuum pump for 2 h. Afterward, the two conductive slides facing each other were separated by a 2 mm thick Teflon frame forming a sandwich, which was filled with a 0.2 M sucrose solution.

Several combinations of voltage, frequency, temperature, and number of cycles were tried to grow the GMPVs without success. Finally, we were able to define a protocol to grow GMPVs where the electroformation swelling chamber was connected to the power generator and submitted to an alternating electric field with a frequency of 10 Hz and a voltage of 4 V for 2 h, followed by 15 min of 5 Hz with 2 V, then by 15 min of 2.5 Hz with 1 V, and, in the last cycle, 30 min of 1 Hz with 1 V. The growth process of GPMVs was carried out in an oven at 40°C to prevent collagen denaturation (Figure 1B).

To verify the presence of proteins in GPMVs, we used the sodium dodecyl-sulfate polyacrylamide gel electrophoresis (SDS-PAGE) technique.[13] Membrane isolate samples were treated with a water: methanol mixture at concentrations of 1:1 to remove lipids from the protein extract. Then, the protein extract was treated with a solution having 50 mM Tris buffer pH 6.8 that contained 2% (w/v) SDS, 0.1% (w/v) bromophenol blue, 10% (w/v) glycerol, and 357 mM 2-mercaptoethanol, and boiled for 5 min to denature the proteins. Thereafter, the sample was run on a 12% polyacrylamide gel, with a 5% stacking gel. For the run, a buffer with 25 mM Tris pH 6.8 containing 250 mM glycine and 0.1% (w/v) SDS was used. The electrophoretic run was performed at a voltage of 100 V, and the gel was developed using Coomassie Brilliant Blue.

Dynamics of photooxidation

For observation under the microscope in phase contrast mode, 100 μL of the solution of each vesicle (either GUV or GPMV) in sucrose was diluted in 600 μL of a 0.2 M glucose solution measured in an osmometer (Osmoma Gonotec 030, Germany) in the presence and absence of MB (50 μM) and with or without light exposure. The observation chamber was filled with the final vesicle solution, ensuring that the osmolarities of the sucrose and glucose solutions were matched to prevent osmotic pressure effects. The slight density difference between the inner and outer solutions causes the vesicles to settle on the bottom slide, making them easier to observe. Additionally, the refractive index difference between the sucrose and glucose solutions enhances contrast when viewing the vesicles under phase contrast microscopy.

Irradiation and observation procedures were performed under a ZEISS Z1 Axiovert 200 inverted optical microscope (Carl Zeiss, Germany) in phase contrast mode, equipped with a Zeiss Axio Cam digital camera (Jena, Germany). From the beginning of the irradiation, a 20 min video was recorded to evaluate the temporal evolution of the membrane under photodynamic action. Irradiation was performed by adapting the microscope's 103 W Hg lamp (HXP 120, Kubler, Carl Zeiss, Germany) with a filter for excitation at $\lambda = 665$ nm, which allowed photoactivation of the MB with a power of approximately 850 μW. Of note, the vesicles used in these experiments were prepared and used on the same day, as they are from natural sources and have low stability.

Changes in GUVs and GPMVs optical contrast associated with membrane permeability increase were analyzed using the ImageJ software as described by Mertins et al.[3] Membrane surface area alterations were evaluated through a routine developed by Prof. Spinozzi's group[14] and inserted as a Macro in ImageJ software.

PDI in *L. amazonensis* promastigote cells

An aliquot of the culture medium solution with the parasites was centrifuged, and the resulting pellet was resuspended in phosphate-buffered saline (PBS) once. The number of *Leishmania* cells was calculated using a Neubauer chamber (approximately 1×10^6 parasites/mL). Then, 100 μL of the solution was pipetted into a quartz chamber and diluted in PBS, in the presence of MB. The chamber was placed under the microscope and irradiated for approximately 27 min. The irradiation was performed using the same procedure as for the GPMVs and GUVs.

RESULTS AND DISCUSSION

The presence of proteins in the isolated membrane was confirmed using SDS-PAGE. Two samples, collected on separate days, were analyzed. As shown, proteins of varying molecular weights were identified in both samples, with no detectable differences between them (Figure 2). Although the protein composition of *Leishmania amazonensis* promastigote membranes may vary slightly depending on the methodology used, our finding is consistent with the label-free proteomics study by Oliveira et al., which identified 95 putative plasma membrane proteins in *L. amazonensis* promastigotes.[15] These proteins were primarily associated

with biological processes such as cell adhesion, signal transduction, and transmembrane transport, as well as molecular functions including transmembrane transporter activity, ATPase activity, lyase activity, and peptidase activity.

In the absence of either MB or light, no morphological changes of mimetic membranes of *L. amazonenis* (GUVs) composed of POPC:POPE:SM:ERG (45:10:15:30) were observed (Figure 3A,B). In contrast, changes in GUVs dispersed in MB were observed under 20 min of irradiation (Figure 3C). As one can note, original spherical vesicles subjected to MB photoactivation immediately start to increase in area and fluctuate after short periods of time to such an extent that buds are released (Figure 3C between 390 and 450 s), followed by a loss of phase contrast between 780 and 900 s (Figure 3C). The maximum area increased to circa 15% and can be explained by the photooxidation of the unsaturated lipids that contain double bonds in the acyl tails and are more susceptible to oxidative stress than saturated lipids.[5]

As previously reported for GUVs composed of just POPC, MB photoactivation generates $^1O_2$ (type II or non-contact mechanism) that reacts with the lipid double bond generating lipid hydroperoxide.[2–4] As the hydroperoxide group is more polar than the hydrophobic tail, it tends to migrate to the membrane surface, imposing an increase in surface area on the order of 15%. Therefore, the hydroperoxidized membrane can show large fluctuations due to excess area, without rupture, as seen in Figure 3C.

The continuity of the lipid peroxidation reaction on POPC-OOH containing membranes occurs due to a type I mechanism of MB (contact dependent).[5] In this, the triplet state of MB reacts with the OOH group formed, abstracting hydrogen and enabling the reaction to continue. Consequently, short-tailed oxidized lipids containing aldehyde can be formed as end product of photooxidation. The presence of these lipids in the membrane increases its permeability, promoting the formation of nanopores and/or macro-pores depending on the extent of lipid oxidation.[3,4] In this case, the formation of nanopores, or sub-micrometric

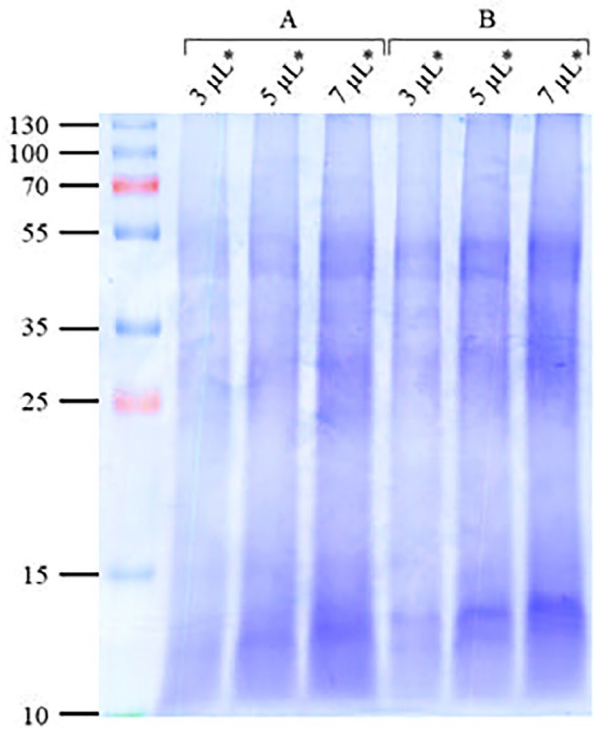

FIGURE 2 SDS-PAGE of two GPMV samples (A and B) obtained on different extraction days. The samples were used in volumes of 3, 5, and 7 µL.

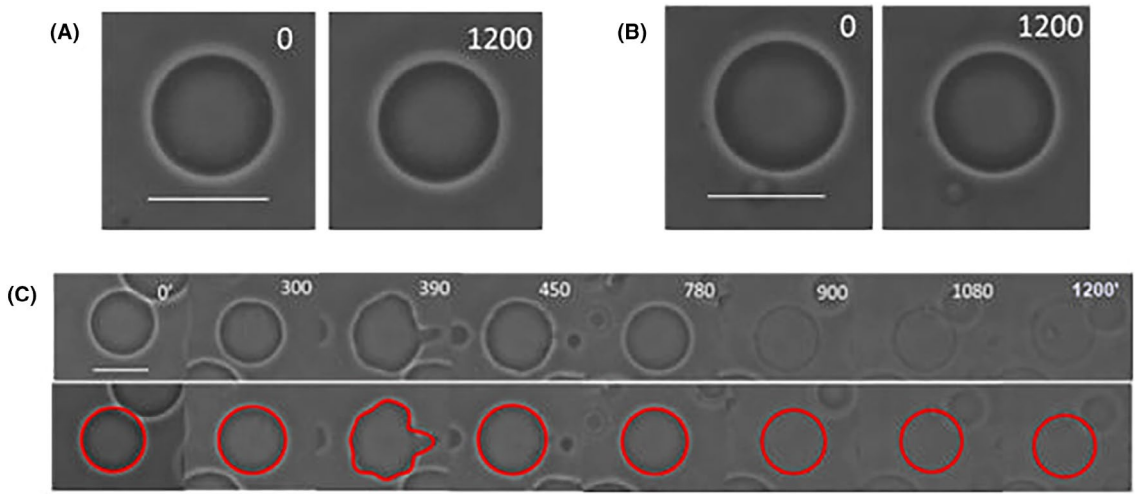

FIGURE 3 Phase contrast optical microscopy of time running sequences (in seconds) of GUVs composed of POPC:POPE:SM:ERG (45:10:15:30 molar ratio) in the presence of MB (50 µM) and absence of light (A); in the absence of MB with red irradiation ($\lambda = 665$ nm) (B); photoactivation of MB (665 nm; 50 µM) (C). The images in each panel above were superimposed with the best contour (red line) surrounding the GUVs, corresponding to the images located below, to calculate the area with an ImageJ macro.[14] Bar spans 20 µm for all snapshots.

pores, allows the exchange of glucose/sucrose solutions in the GUVs, decreasing their optical contrast.

Figure 4 presents the phase contrast decrease with MB irradiation time for GUVs and GPMVs. Of note, the permeability increase in the mimetic *Leishmania* membrane occurs more slowly than in the pure POPC membrane, which loses optical contrast in approximately 250 s.[3] Additionally, neither the pure POPC nor the *Leishmania* mimetic membranes exhibited rupture, even after 20 min of irradiation. Here, the presence of the unsaturated lipid SM in the model membrane as well as ERG, which is another target of $^1O_2$ attack, may impair the membrane dynamic response to oxidative stress insult.

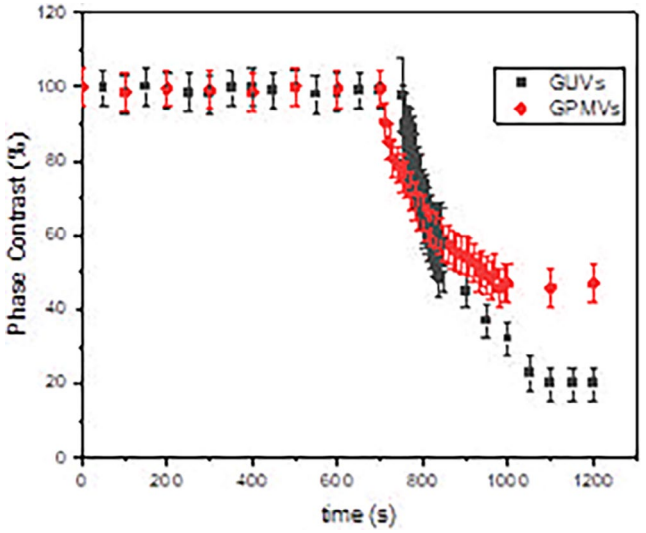

FIGURE 4 Optical phase contrast loss of giant vesicles under MB irradiation (665 nm; 50 μM) for mimetic GUVs of POPC:POPE:SM:ERG (45:10:15:30 molar ratio) and GPMVs reconstituted from *L. amazonensis* promastigote cells.

Regarding GPMVs, no membrane damage was observed under the effect of MB alone (Figure 5A) or light alone (Figure 5B). When MB was combined with red light, no changes in membrane morphology or alterations in surface area were detected. Interestingly, although the loss of optical contrast began approximately 50 s earlier than in GUVs, a lower loss of optical contrast (~55%) is noticed (Figures 4 and 5C). This suggests that only partial membrane permeabilization was achieved after 1200 s of irradiation, with no membrane rupture observed.

As discussed earlier, phase contrast loss results from ROS generation, which primarily targets unsaturated lipid acyl chains in the membrane, leading to pore formation and the exchange of internal (sucrose) and external (glucose) solutions. However, under photooxidation, GUVs and GPMVs exhibited distinct behaviors in terms of optical contrast loss (see Figure 4). In GUVs, composed solely of lipids, photooxidation caused an increase in membrane area followed by a significant loss of contrast. In contrast, GPMVs, which contain embedded proteins, displayed less pronounced optical contrast loss without any accompanying membrane expansion. This suggests that the presence of proteins in GPMVs can help to stabilize the membrane, thus altering their response to oxidative stress. Unlike GUVs, the protein-rich GPMVs seem more resistant to membrane reshaping, highlighting the role that proteins play in modulating the effects of photooxidation.

Additionally, both lipids and proteins are susceptible to oxidative damage, and their interaction with ROS could create a dynamic where they "compete" for these oxidative agents. While the effects of photooxidation on

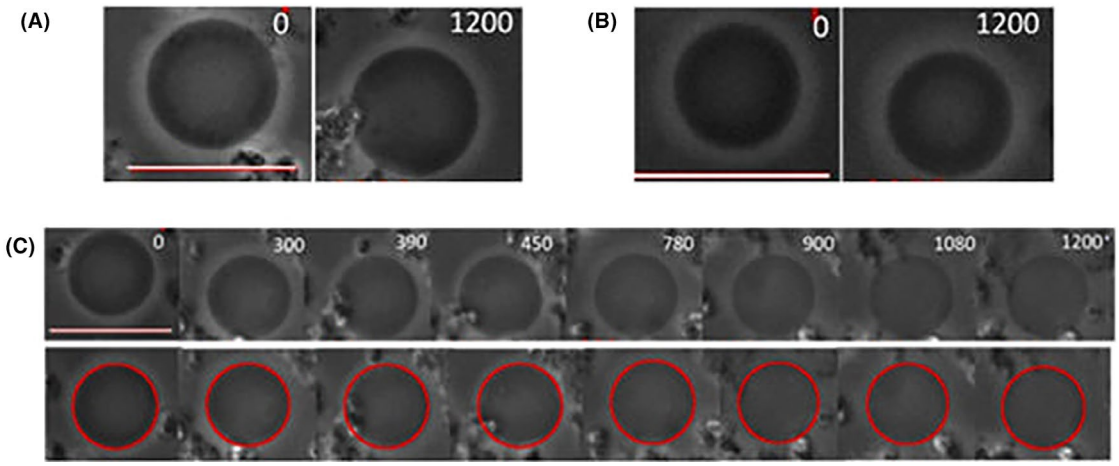

FIGURE 5 Images of GPMVs reconstituted from *L. amazonensis* promastigote cells with MB (50 μM) without irradiation (A); in the absence of MB with red irradiation ($\lambda = 665$ nm) (B); photoactivation of MB (665 nm; 50 μM) (C). The images in each panel above were superimposed with the best contour (red line) surrounding the GPMVs, corresponding to the images located below. Bar spans 20 μm for all snapshots.

GPMVs are still not well explored, it is known that ROS can oxidize amino acid chains and disrupt protein structure, potentially leading to protein fragmentation. Among the amino acids, cysteine and methionine are particularly susceptible to oxidation due to the high reactivity of their sulfur groups, making them especially vulnerable to oxidative modifications.[16]

The rate constants for the reaction of $^1O_2$ with amino acid residues are on the order of 10^6–$10^7\,M^{-1}s^{-1}$,[17] indicating a high reactivity of $^1O_2$ with proteins. In contrast, for lipids such as POPC, the rate constant was calculated as $3\times10^6\,M^{-1}s^{-1}$.[18] This difference in reactivity (potentially up to an order of magnitude) suggests that proteins can be more prone to oxidation by $^1O_2$ than lipids. As a result, we hypothesize that in systems containing both proteins and lipids, such as GPMVs, proteins may undergo oxidation more rapidly than lipids, leading to an earlier onset (around 50 s) of contrast loss compared to GUVs (see Figure 4), where lipids dominate the composition. This faster reaction with proteins could be a key factor in the observed differential behavior between GPMVs and GUVs under photooxidative conditions. Indeed, while proteins oxidize more quickly than lipids, the oxidation of proteins often involves specific sites and may not necessarily lead to complete membrane destabilization, as some structural integrity may remain intact. On the other hand, mimetic membranes (which lack proteins) might undergo more uniform damage, leading to a more significant loss of optical contrast due to the absence of protective or stabilizing factors.

Conversely, we cannot overlook the possibility that certain membrane proteins may act as antioxidants. Lipid peroxidation progresses through three key stages: initiation, propagation, and termination. Given that lipid peroxidation occurs near high concentrations of membrane-embedded proteins with exposed hydrophobic amino acid side chains, we assume that intramembrane tyrosine and tryptophan residues may serve as chain-breaking antioxidants, thereby inhibiting the process. This hypothesis is supported by the reaction rate constant of lipid peroxyl radicals with tyrosine and tryptophan, which is approximately 10^4–$10^5\,M^{-1}s^{-1}$.[19]

Lastly, we monitored *L. amazonensis* cells under PDI using 50 μM MB and red light at 830 μW (as previously used), tracking their dynamics in real time. Despite challenges in focusing due to the motility of the parasites, we observed significant morphological changes and cessation of movement after 27 min of irradiation (Figure 6, Supporting Information S1). Initially fusiform, the *Leishmania* promastigotes transitioned to a rounded shape in response to oxidative stress induced by the treatment, likely leading to apoptosis.[20]

Despite clear evidence of apoptosis in *Leishmania*, its mechanisms remain poorly understood. This is primarily because key proteins involved in mammalian apoptosis, such as caspases, have not been identified in *Leishmania*. However, recent research has uncovered several proteins that appear to play a role in *Leishmania* cell death.[21]

Furthermore, recent findings suggest that protein degradation is the primary driver, rather than a consequence, of MB-mediated PDI in bacterial cells.[22] The study demonstrated that protein degradation follows a dose-dependent trend closely aligned with bacterial inactivation kinetics, suggesting it is a more significant factor compared to membrane permeabilization and DNA damage. Thus, it appears that proteins indeed play a critical role in PDI.

In conclusion, this study represents a first step toward understanding the role of proteins in the photooxidation of GPMVs. The electroformation technique, combined with the protocol developed here, successfully generated GPMVs from *L. amazonensis* promastigote membrane isolates, which may also serve as potential drug delivery systems for visceral leishmaniasis treatment.[23] Additionally, the membrane isolation method effectively extracted the parasite's membrane while preserving its

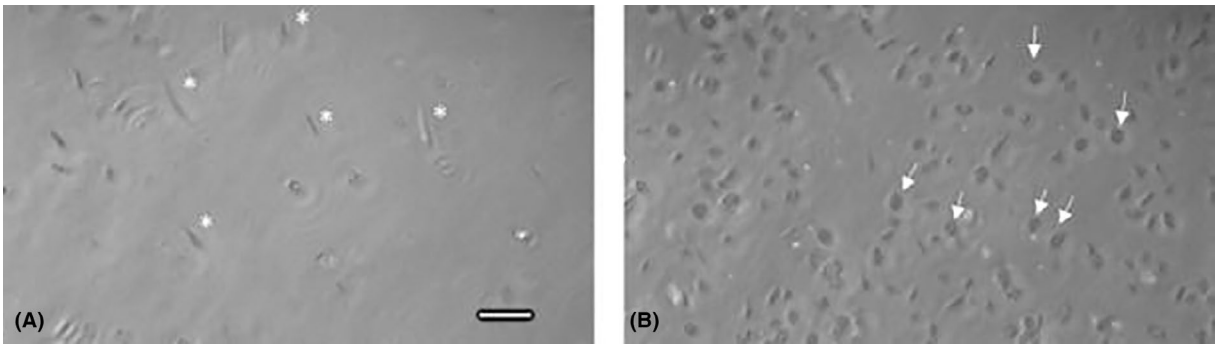

FIGURE 6 *L. amazonensis* promastigote cells undergoing PDI with MB at 50 μM and irradiation at $\lambda = 665$ nm, $p = 830$ μW. Note the fusiform shape of the cells at the start of irradiation (*) (A). After 27 min of irradiation, the parasites cease movement and adopt a rounded shape (arrows) (B). The bar spans 20 μm.

lipid and protein components. Photoactivation of MB in mimetic GUVs induced a clear photooxidation effect, initially increasing the membrane area before stabilization and a significant loss of optical contrast. In contrast, GPMVs exhibited less contrast loss than mimetic GUVs and showed no reshaping, suggesting that the presence of proteins in GPMVs modifies the photoresponse to oxidative stress. Further studies are needed to elucidate the molecular mechanisms underlying the photooxidation of natural GPMVs, and we hope our findings will motivate future research in this field.

ACKNOWLEDGMENTS

The authors wish to express their gratitude to Dr. Fernanda V. Cabral and Dr. Ismael P. Sauter for their technical assistance, as well as to Dr. Caetano P. Sabino for the insightful discussions. This study was financed in part by the Coordenação de Aperfeiçoamento de Pessoal de Nível Superior—Brasil (CAPES)—Finance Code 001. MSR acknowledges Comissão Nacional de Energia Nuclear (CNEN) and Conselho Nacional de Desenvolvimento Científico e Tecnológico (CNPq, grant # 465763/2014-6) for financial support. RI, PC, and MSR hold research fellowships from the CNPq. The Article Processing Charge for the publication of this research was funded by the Coordenação de Aperfeiçoamento de Pessoal de Nível Superior - Brasil (CAPES) (ROR identifier: 00x0ma614).

CONFLICT OF INTEREST STATEMENT

The authors have no competing interests to declare.

DATA AVAILABILITY STATEMENT

The data will be available upon reasonable request.

ORCID

Martha S. Ribeiro https://orcid.org/0000-0002-4203-1134

REFERENCES

1. Cabral FV, dos Santos Souza TH, Sellera FP, Fontes A, Ribeiro MS. Strengthening collaborations at the biology-physics interface: trends in antimicrobial photodynamic therapy. *Biophys Rev*. 2023;15:685-697. doi:10.1007/S12551-023-01066-5
2. Itri R, Junqueira HC, Mertins O, Baptista MS. Membrane changes under oxidative stress: the impact of oxidized lipids. *Biophys Rev*. 2014;6:47-61. doi:10.1007/s12551-013-0128-9
3. Mertins O, Bacellar IO, Thalmann F, Marques CM, Baptista MS, Itri R. Physical damage on giant vesicles membrane as a result of methylene blue photoirradiation. *Biophys J*. 2014;106:162-171. doi:10.1016/j.bpj.2013.11.4457
4. Tsubone TM, Baptista MS, Itri R. Understanding membrane remodelling initiated by photosensitized lipid oxidation. *Biophys Chem*. 2019;254:106263. doi:10.1016/j.bpc.2019.106263
5. Bacellar IOL, Baptista MS. Mechanisms of photosensitized lipid oxidation and membrane permeabilization. *ACS Omega*. 2019;4:21636-21646. doi:10.1021/ACSOMEGA.9B03244
6. Cabral FV, Souza TH d S, Sellera FP, Fontes A, Ribeiro MS. Towards effective cutaneous leishmaniasis treatment with light-based technologies. A systematic review and meta-analysis of preclinical studies. *J Photochem Photobiol B Biol*. 2021;221:112236. doi:10.1016/j.jphotobiol.2021.112236
7. Ullah N, Sagar M, Abidin Z u, Naeem MA, Din SZU, Ahmad I. Photodynamic therapy in management of cutaneous leishmaniasis: a systematic review. *Lasers Med Sci*. 2024;39:226. doi:10.1007/S10103-024-04174-0
8. Corman HN, McNamara CW, Bakowski MA. Drug discovery for cutaneous leishmaniasis: a review of developments in the past 15 years. *Microorganisms*. 2023;11:2845. doi:10.3390/MICROORGANISMS11122845
9. Zhang K, Beverley SM. Phospholipid and sphingolipid metabolism in leishmania. *Mol Biochem Parasitol*. 2009;170:55. doi:10.1016/J.MOLBIOPARA.2009.12.004
10. Young SA, Roberts MD, Smith TK. The importance of targeting lipid metabolism in parasites for drug discovery. *Comprehensive Analysis of Parasite Biology: From Metabolism to Drug Discovery*. Wiley; 2016:343-369.
11. Angelova MI, Dimitrov DS. Liposome electroformation. *Faraday Discuss Chem Soc*. 1986;81:303-311. doi:10.1039/DC9868100303
12. Mukherjee T, Mandal D, Bhaduri A. Leishmania plasma membrane Mg2+-ATPase is a H+/K+-antiporter involved in glucose symport. studies with sealed ghosts and vesicles of opposite polarity. *J Biol Chem*. 2001;276:5563-5569. doi:10.1074/jbc.M008469200
13. Santos FR, Ferraz DB, Daghastanli KRP, Ramalho-Pinto FJ, Ciancaglini P. Mimetic membrane system to carry multiple antigenic proteins from leishmania amazonensis. *J Membr Biol*. 2006;210:173-181. doi:10.1007/S00232-006-0005-6
14. Marega Motta A, Donato M, Mobbili G, Mariani P, Itri R, Spinozzi F. Unveiling the mono-rhamnolipid and di-rhamnolipid mechanisms of action upon plasma membrane models. *J Colloid Interface Sci*. 2022;624:579-592. doi:10.1016/J.JCIS.2022.05.145
15. Oliveira IHR, Figueiredo HCP, Rezende CP, et al. Assessing the composition of the plasma membrane of Leishmania (Leishmania) infantum and L. (L.) amazonensis using label-free proteomics. *Exp Parasitol*. 2020;218:107964. doi:10.1016/J.EXPPARA.2020.107964
16. Zhang W, Xiao S, Ahn DU. Protein oxidation: basic principles and implications for meat quality. *Crit Rev Food Sci Nutr*. 2013;53:1191-1201. doi:10.1080/10408398.2011.577540
17. Fuentes-Lemus E, López-Alarcón C. Photo-induced protein oxidation: mechanisms, consequences and medical applications. *Essays Biochem*. 2020;64:33-44. doi:10.1042/EBC20190044
18. Weber G, Charitat T, Baptista MS, et al. Lipid oxidation induces structural changes in biomimetic membranes. *Soft Matter*. 2014;10:4241-4247. doi:10.1039/c3sm52740a
19. Hajieva P, Abrosimov R, Kunath S, Moosmann B. Antioxidant and prooxidant modulation of lipid peroxidation by integral membrane proteins. *Free Radic Res*. 2023;57:105-114. doi:10.1080/10715762.2023.2201391

20. Aureliano DP, Lindoso JAL, de Castro Soares SR, Takakura CFH, Pereira TM, Ribeiro MS. Cell death mechanisms in leishmania amazonensis triggered by methylene blue-mediated antiparasitic photodynamic therapy. *Photodiagn Photodyn Ther*. 2018;23:1-8. doi:10.1016/j.pdpdt.2018.05.005
21. Basmaciyan L, Casanova M. Cell death in leishmania. *Parasite*. 2019;26:71. doi:10.1051/PARASITE/2019071
22. Sabino CP, Ribeiro MS, Wainwright M, et al. The biochemical mechanisms of antimicrobial photodynamic therapy†. *Photochem Photobiol*. 2023;99:742-750. doi:10.1111/PHP.13685
23. Jokhadar ŠZ, Klancnik U, Grundner M, et al. GPMVs in variable physiological conditions: could they be used for therapy delivery? *BMC Biophys*. 2018;11:1-12. doi:10.1186/S13628-017-0041-X

SUPPORTING INFORMATION

Additional supporting information can be found online in the Supporting Information section at the end of this article.

How to cite this article: de Souza MDF, Ciancaglini P, Itri R, Ribeiro MS. Developing giant plasma membrane vesicles from *Leishmania* cells to investigate the role of membrane proteins in photodynamic inactivation. *Photochem Photobiol*. 2025;00:1-9. doi:10.1111/php.70000